Paper presentation

nature communications

Article

https://doi.org/10.1038/s41467-024-45234-x

Observing growth and interfacial dynamics of nanocrystalline ice in thin amorphous ice films

Received: 6 July 2023

Accepted: 16 January 2024

Published online: 30 January 2024

Minyoung Lee[1,2,10], Sang Yup Lee[3,4,5,10], Min-Ho Kang[6,7,10], Tae Kyung Won[3,5], Sungsu Kang[1,2], Joodeok Kim[1,2], Jungwon Park[1,2,8,9] ✉ & Dong June Ahn[3,4,5] ✉

[1]School of Chemical and Biological Engineering, and Institute of Chemical Processes, Seoul National University, Seoul 08826, Republic of Korea. [2]Center for Nanoparticle Research, Institute of Basic Science (IBS), Seoul 08826, Republic of Korea. [3]Department of Chemical and Biological Engineering, Korea University, Seoul 02841, Republic of Korea. [4]KU-KIST Graduate school of Converging Science and Technology, Korea University, Seoul 02841, Republic of Korea. [5]The w:i Interface Augmentation Center, Korea University, Seoul 02841, Republic of Korea. [6]Department of Biomedical-Chemical Engineering, The Catholic University of Korea, Bucheon-si 14662, Republic of Korea. [7]Department of Biotechnology, The Catholic University of Korea, Bucheon-si 14662, Republic of Korea. [8]Institute of Engineering Research, College of Engineering, Seoul National University, Seoul 08826, Republic of Korea. [9]Advanced Institutes of Convergence Technology, Seoul National University, Suwon-si 16229, Republic of Korea. [10]These authors contributed equally: Minyoung Lee, Sang Yup Lee, Min-Ho Kang. ✉e-mail: jungwonpark@snu.ac.kr; ahn@korea.ac.kr

Bijesh

31-08-2024

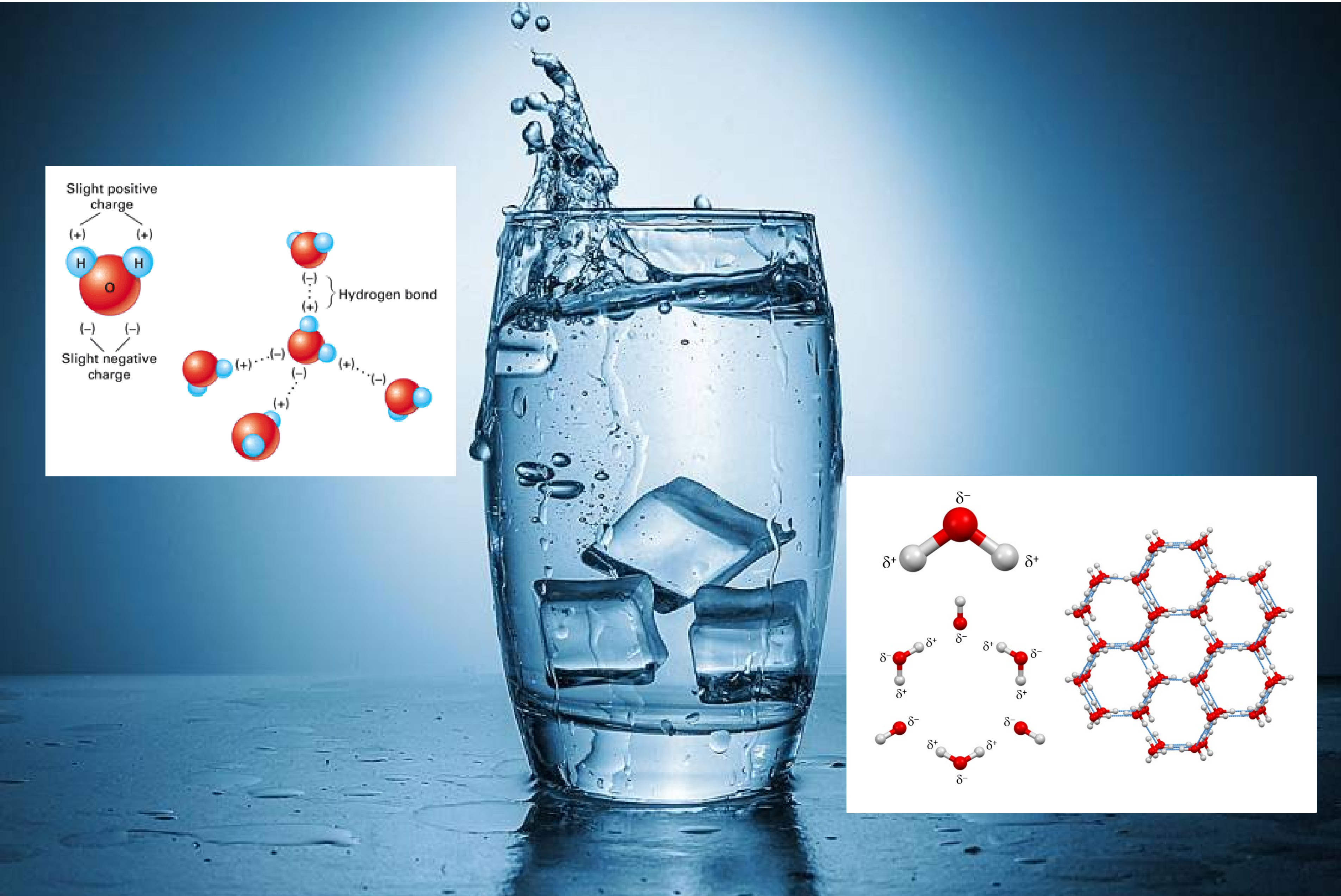

Slight positive charge
(+)
(+)
H
H
O
(–)
(–)
Slight negative charge
(–)
(+)
Hydrogen bond
(+)
(–)
(–)
(+)
(–)
(+)
δ−
δ+
δ+
δ+
δ−
δ+
δ−
δ+
δ+
δ+
δ−
δ−
δ+
δ+
δ−

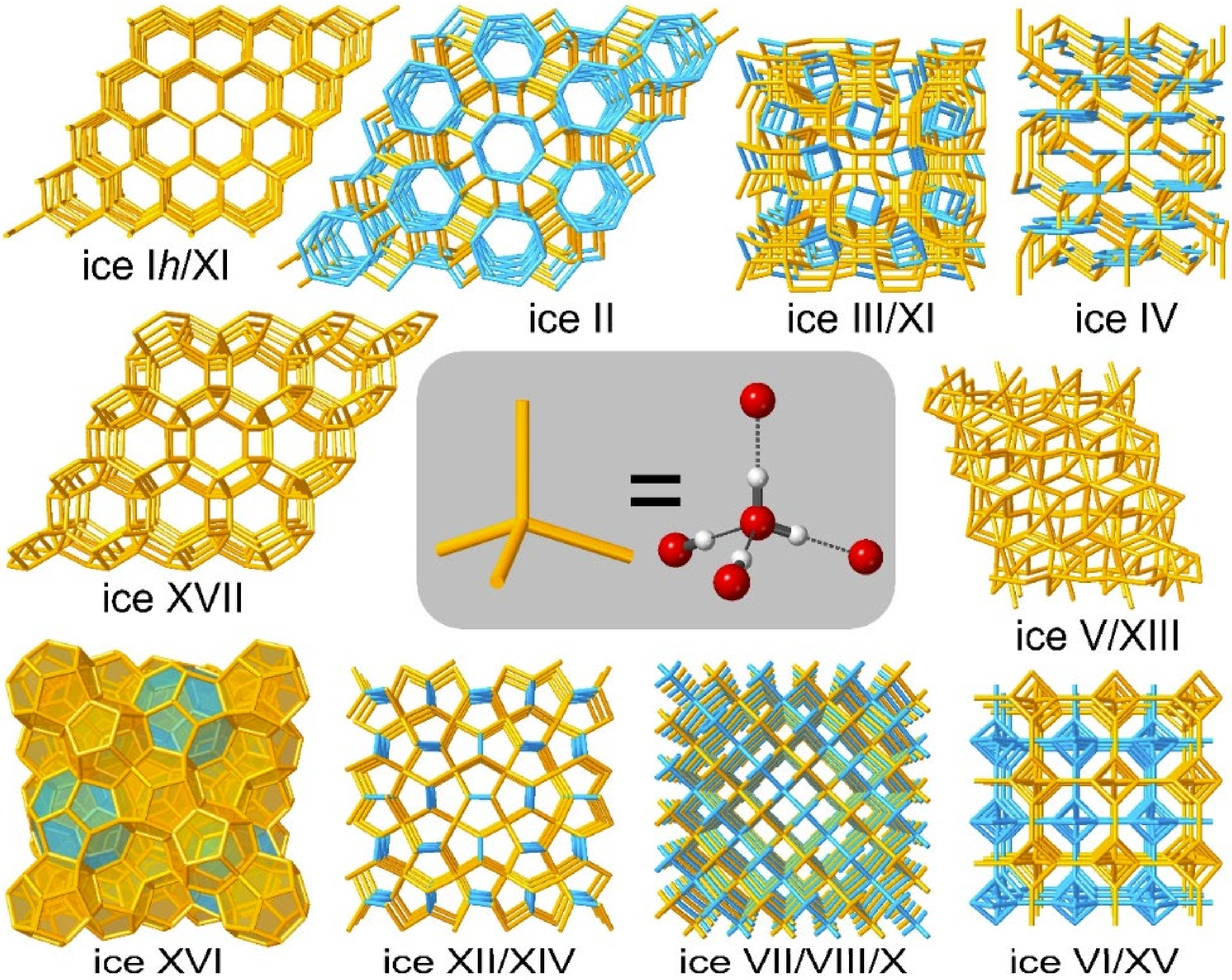
ice Ih/XI
ice II
ice III/XI
ice IV
ice XVII
=
ice V/XIII
ice XVI
ice XII/XIV
ice VII/VIII/X
ice VI/XV
−250 °C
−200 °C
−150 °C
−100 °C
−50 °C
0 °C
50 °C
100 °C
150 °C
200 °C
250 °C
300 °C
350 °C

Relationships and transformations between the amorphous ices

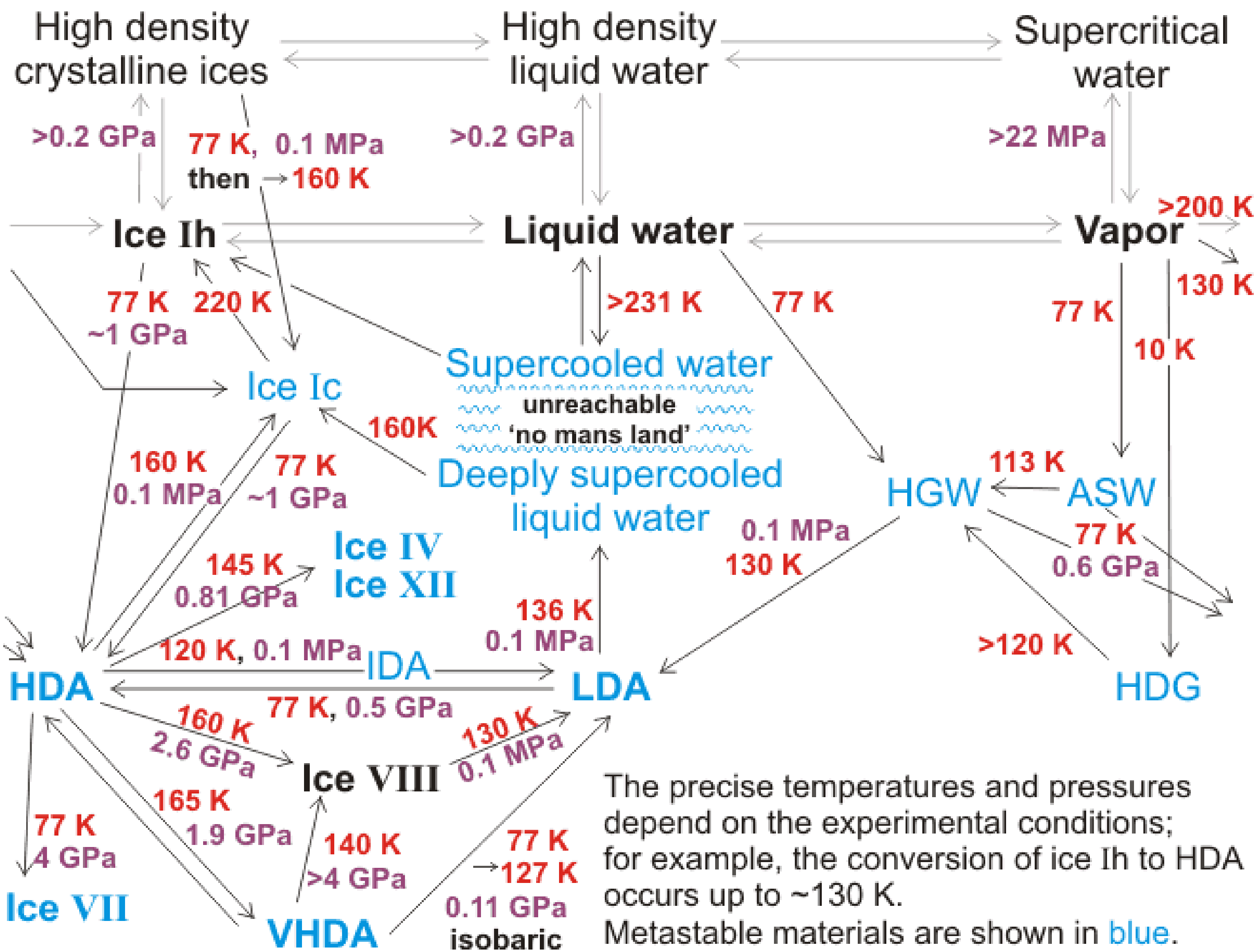

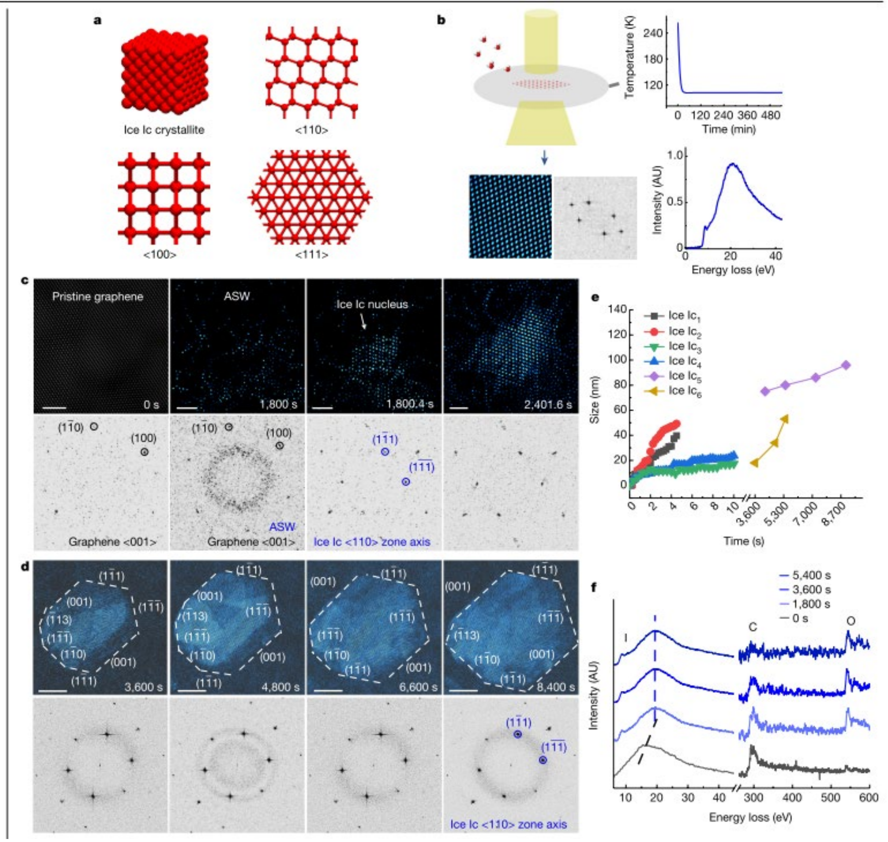

Nature. 2023 May 4;617:86-91

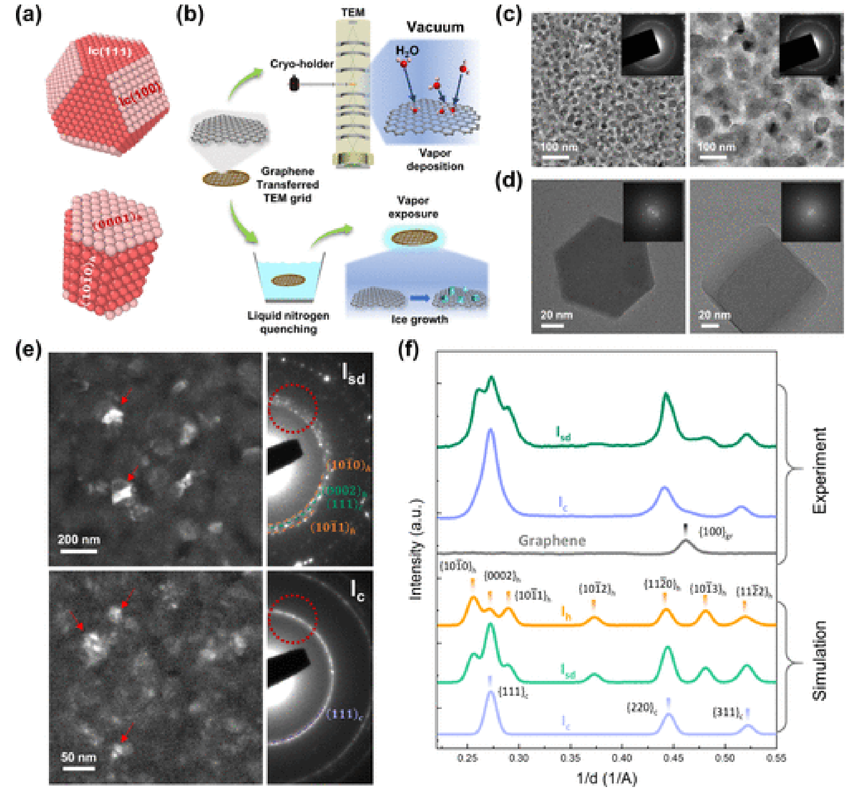

Nano Lett. 2024, XXXX, XXX, XXX-XXX

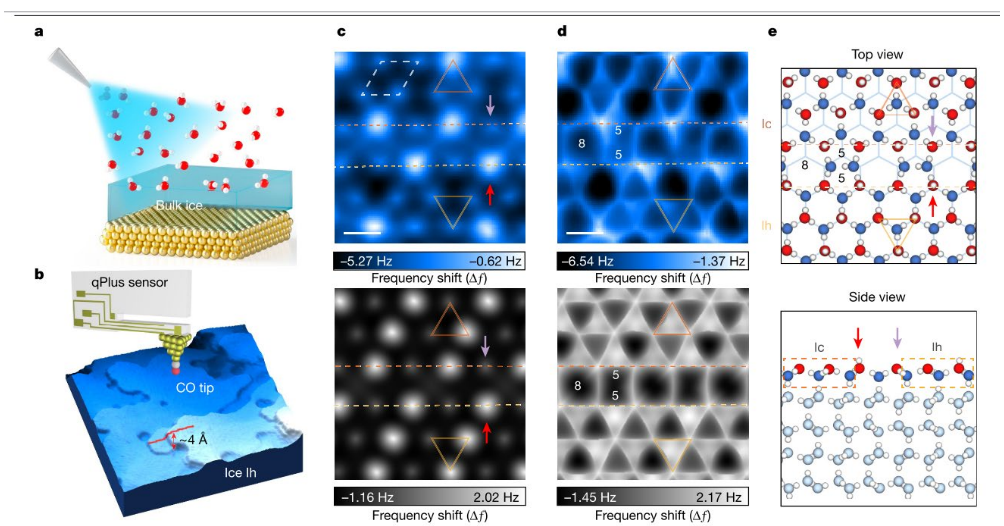

Nature. 2024 May 22;1;630, 375–380

nature communications

Article https://doi.org/10.1038/s41467-024-45234-x

Observing growth and interfacial dynamics of nanocrystalline ice in thin amorphous ice films

Received: 6 July 2023

Accepted: 16 January 2024

Published online: 30 January 2024

Minyoung Lee[1,2,10], Sang Yup Lee[3,4,5,10], Min-Ho Kang[6,7,10], Tae Kyung Won[3,5], Sungsu Kang[1,2], Joodeok Kim[1,2], Jungwon Park[1,2,8,9] & Dong June Ahn[3,4,5]

- **Amorphous ice film preparation**
- **Energy-filtered transmission electron microscopy for measuring ice thickness**
- **Ice characterization with electron diffraction**
- **Results and discussions**

Amorphous ice film preparation

Glow discharging Sample application Sample removal Vitrification

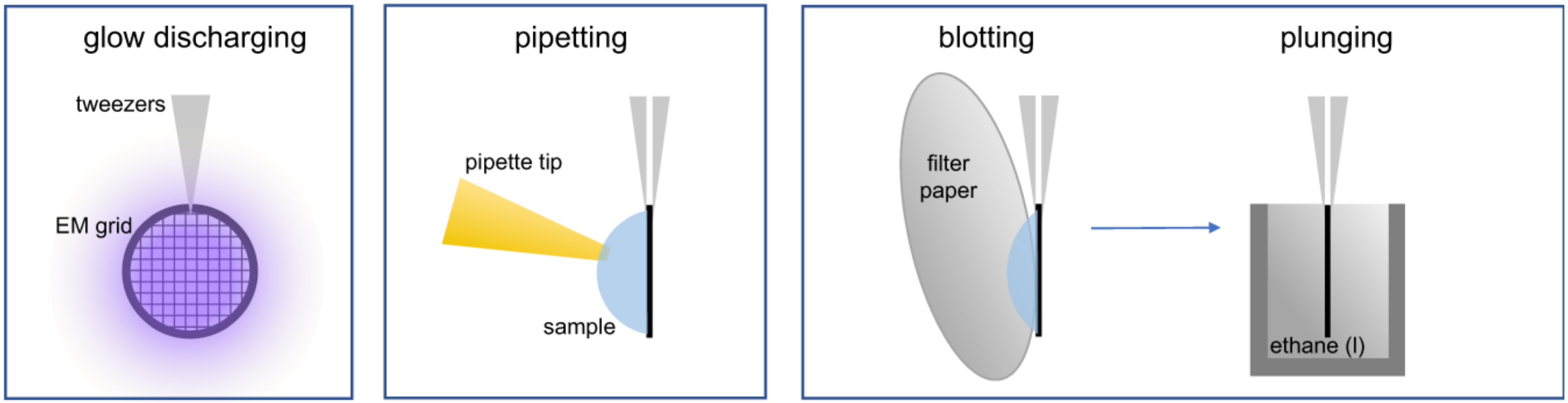

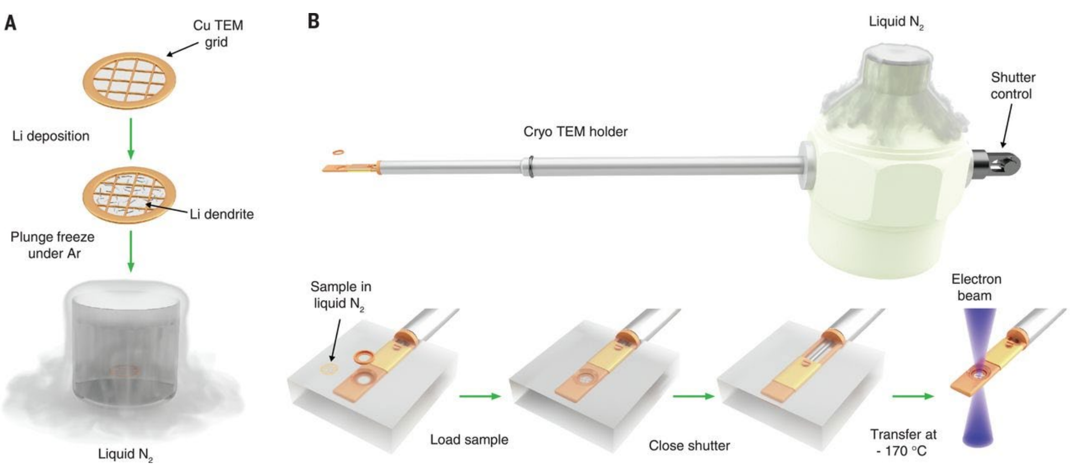

*Science,*358,506-510(**2017**)

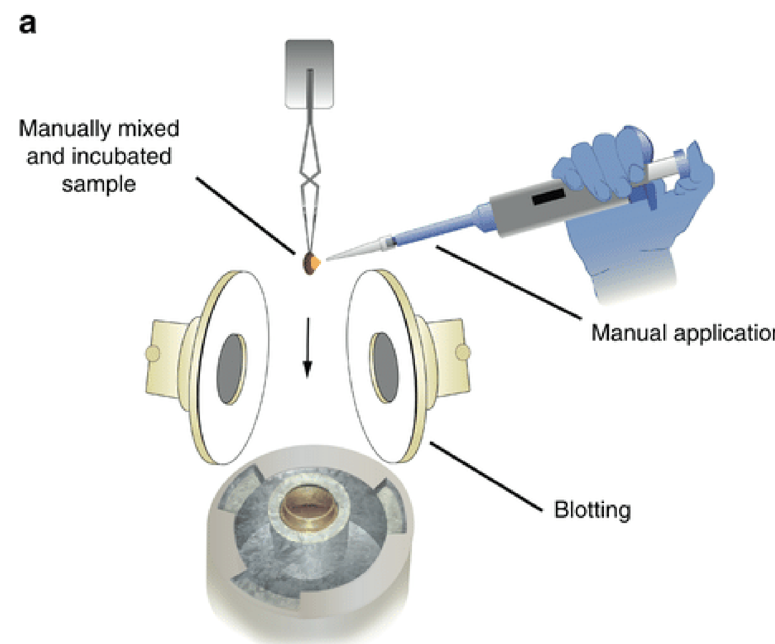

Traditional grid preparation

Energy-filtered transmission electron microscopy for measuring ice thickness

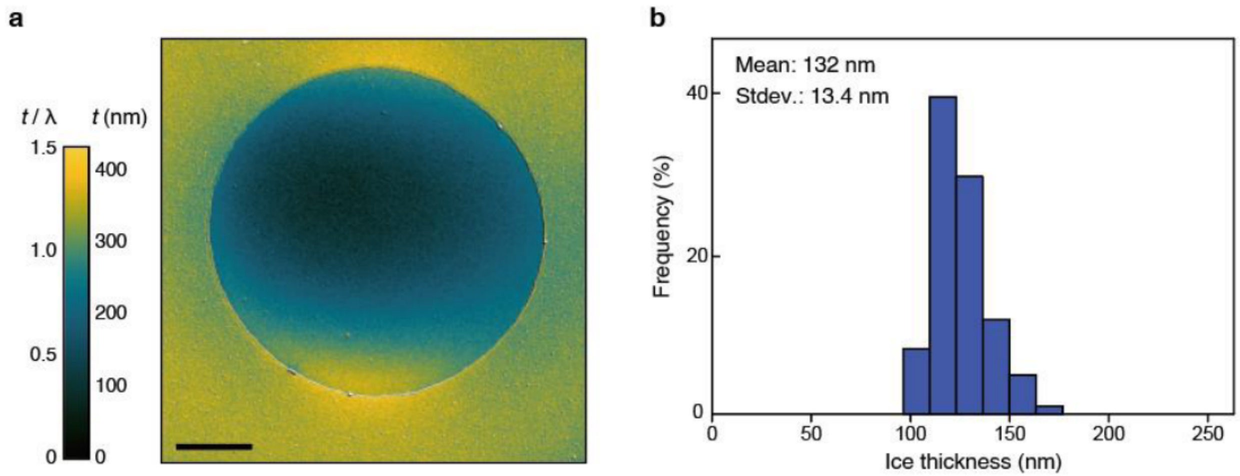

Supplementary Fig. 1: EFTEM analysis for amorphous ice thickness measurement.
a EFTEM image of a carbon film hole with a free-standing amorphous ice film in the region inside the hole (Scale bar = 200 nm). Each pixel is color-mapped based on *t*/λ values. The thickness *t* is calculated based on the inelastic mean free path value of ice 287 nm at 200 keV.
b Histogram of ice thickness values obtained for each pixel located inside holes, taken from multiple holes.

$$\frac{t}{\lambda} = -\ln\left(\frac{I_0}{I_t}\right)$$

where t is the sample thickness, λ is the inelastic mean free path of the sample, and I_0 and I_t are the zero-loss intensities and the total intensities respectively. The inelastic mean free path value for ice at 200 keV, which is 287 nm

Ice characterization with electron diffraction

$$Q(\text{Å}^{-1}) = \frac{2\pi k(\text{nm}^{-1})}{10(\text{nm}^{-1}/\text{Å}^{-1})}$$

$$2\theta(\text{deg}) = 2^{*}\sin^{-1}\left(\frac{Q\lambda}{4\pi}\right)$$

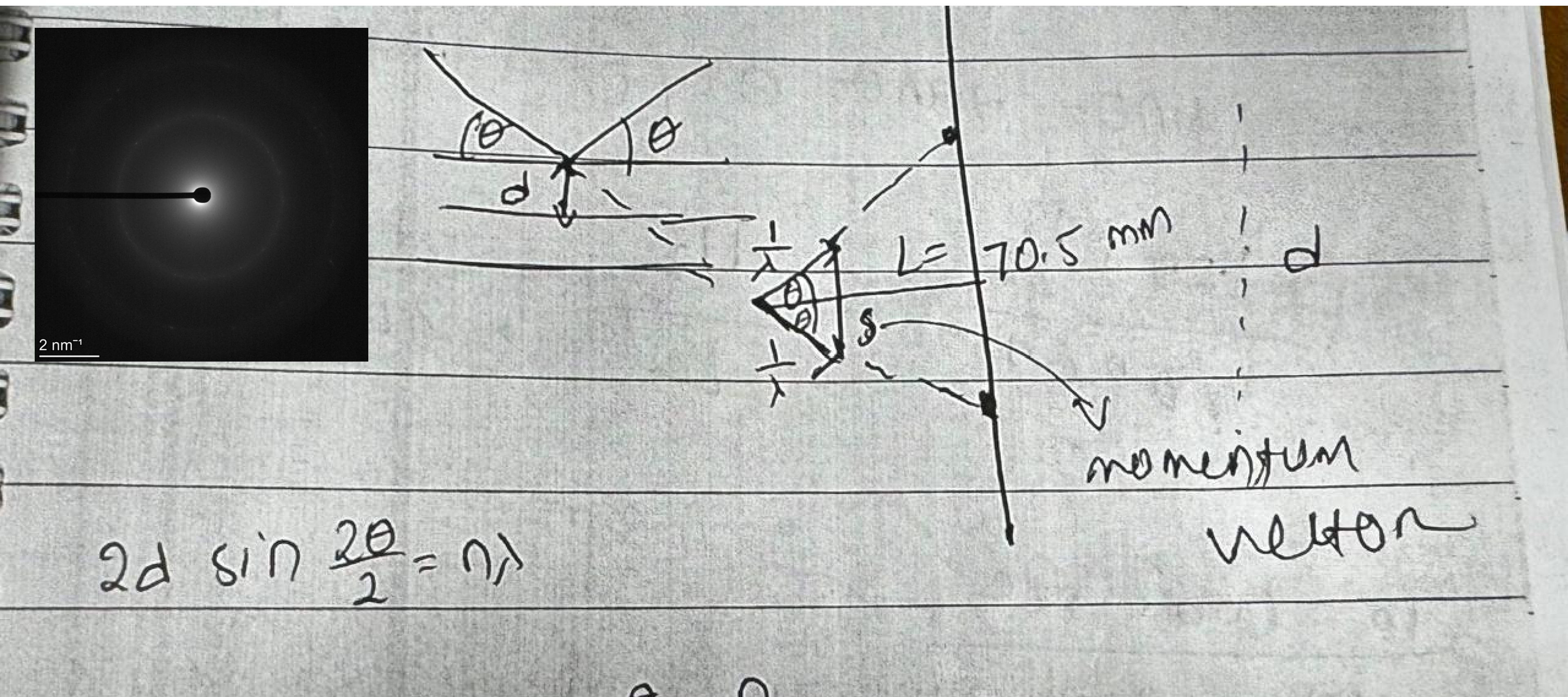

Image processing and nanocrystal quantification

ImageJ
MATLAB

Growth of nanocrystalline ice from amorphous ice

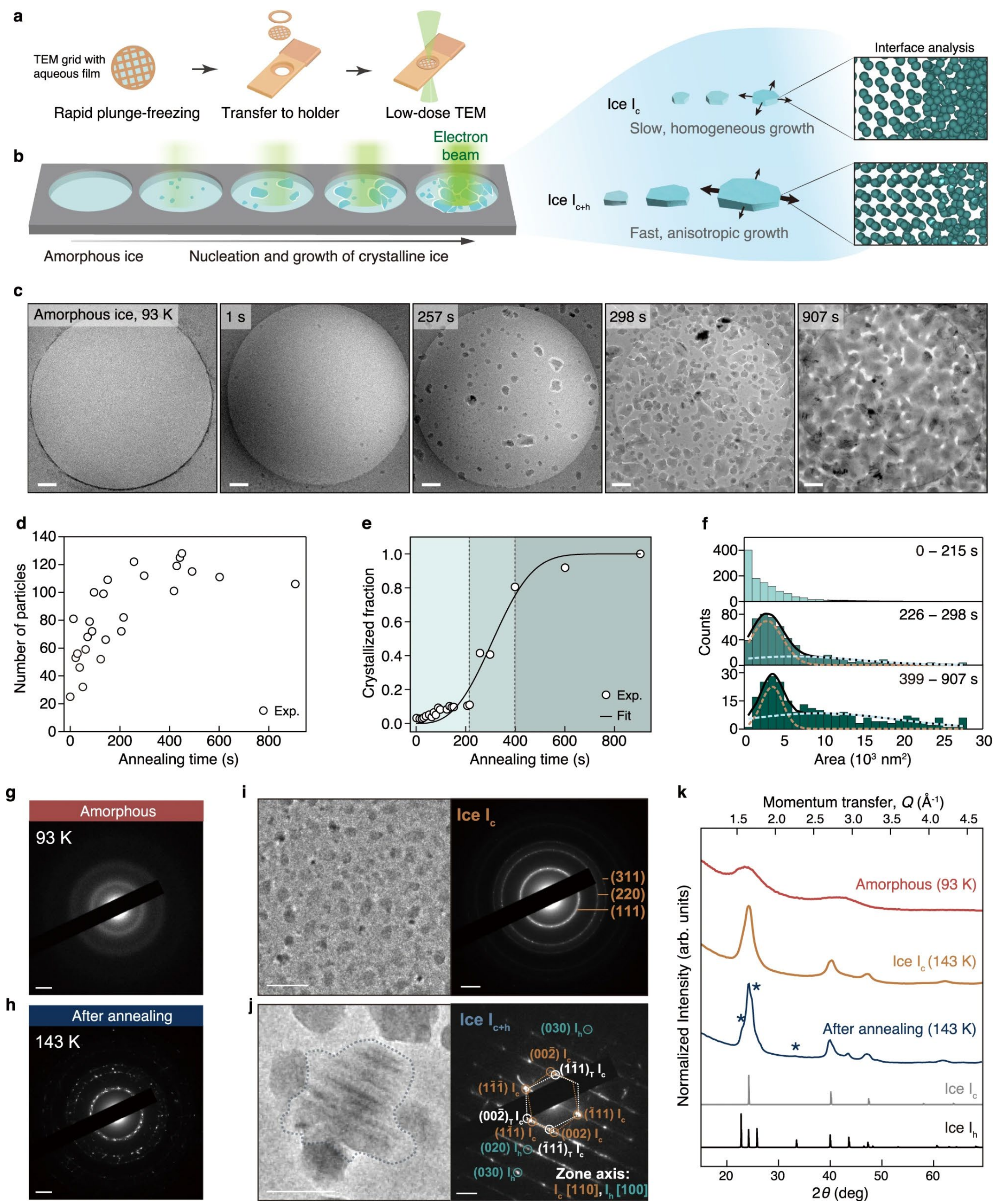

The structure of the ice I_{c+h} domain

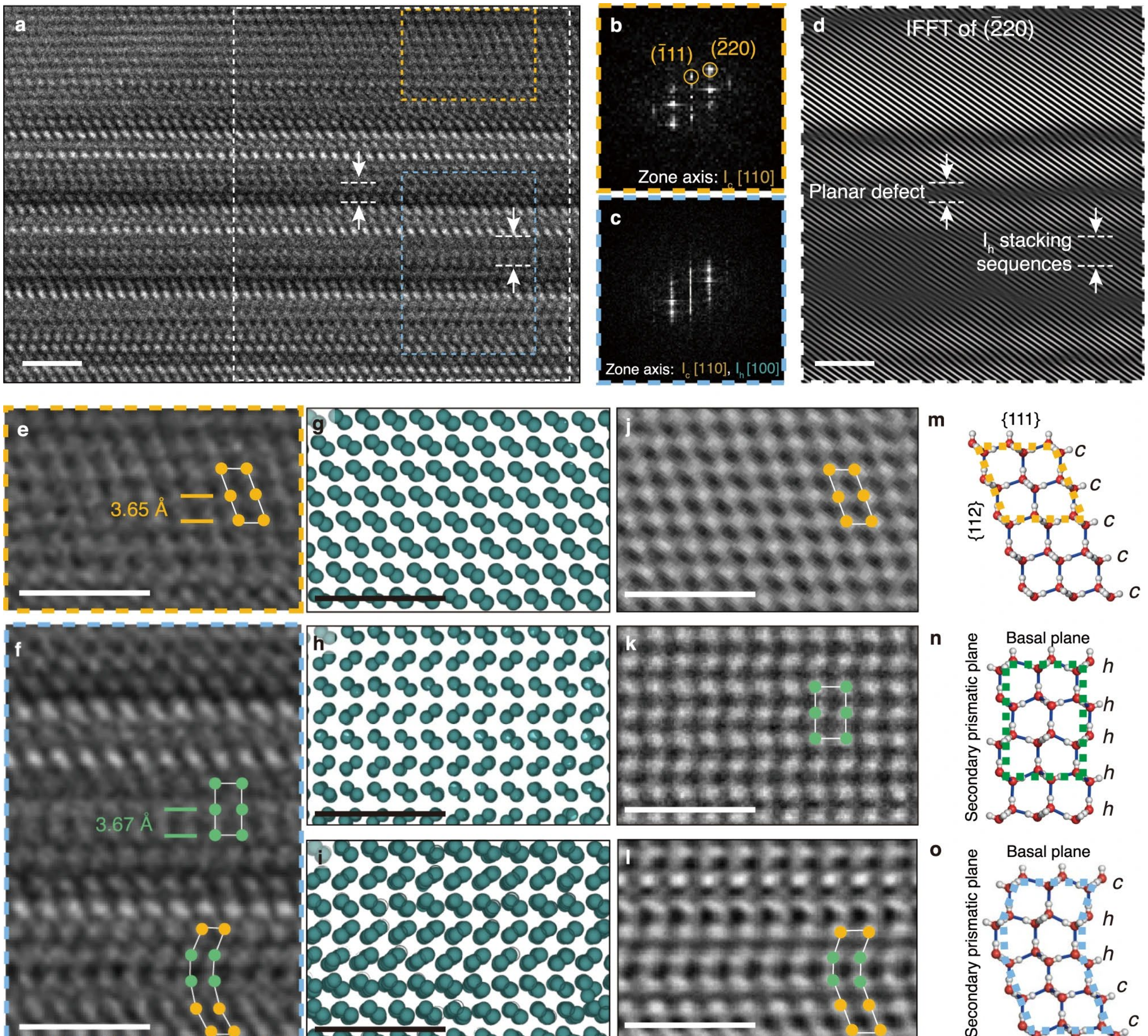

Growth dynamics of ice nanocrystal polymorphs

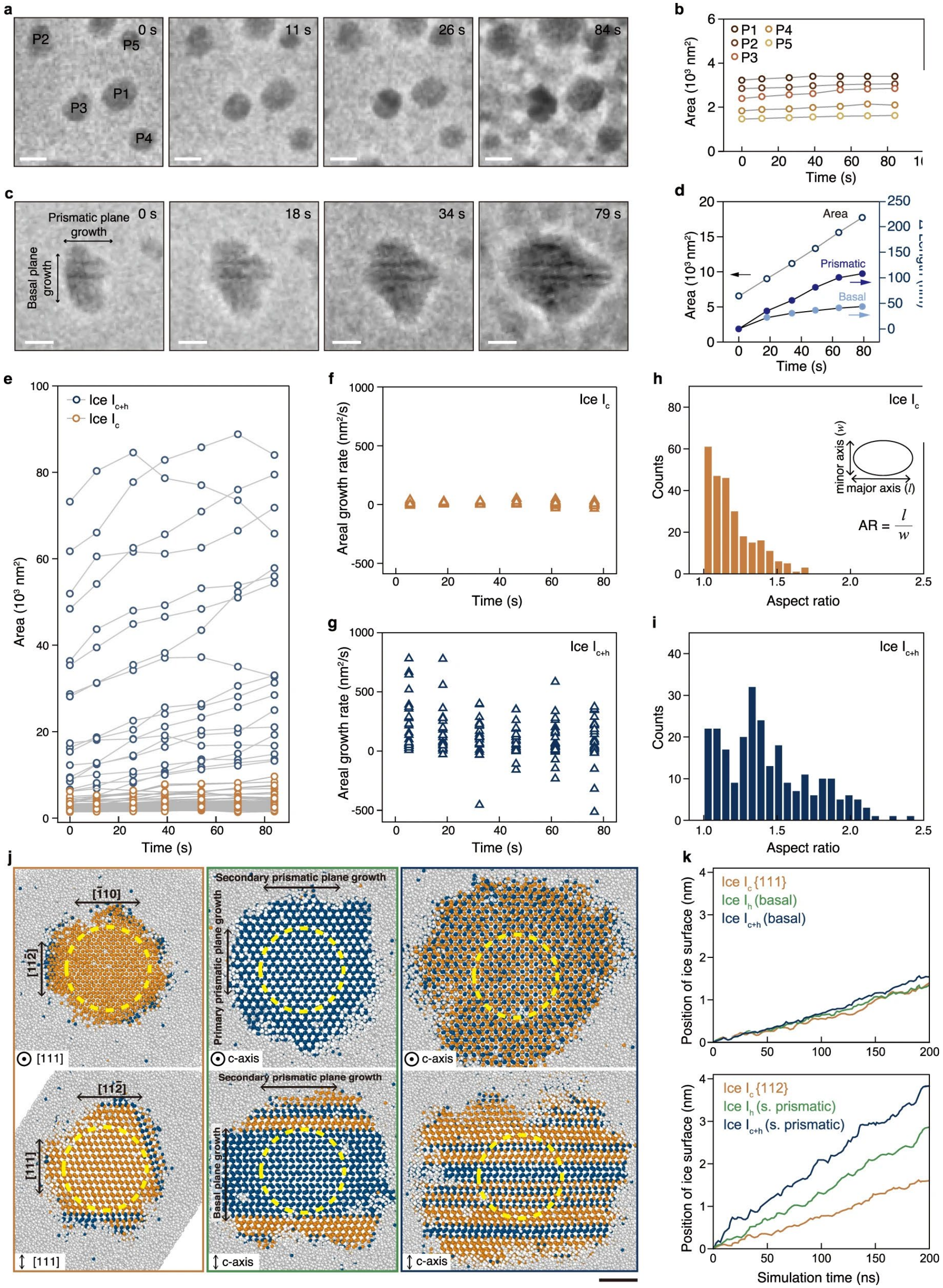

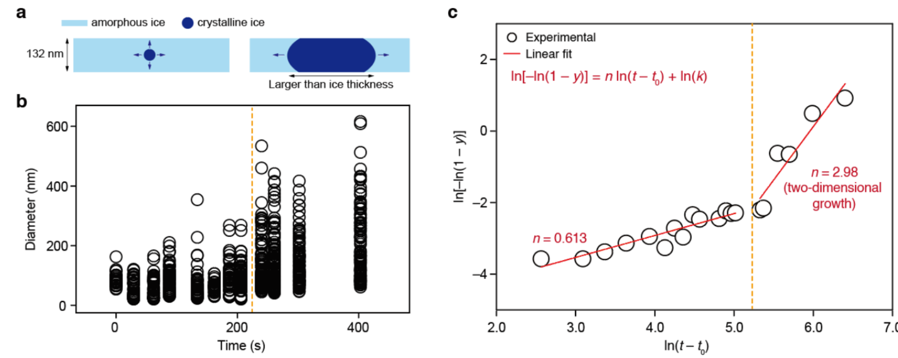

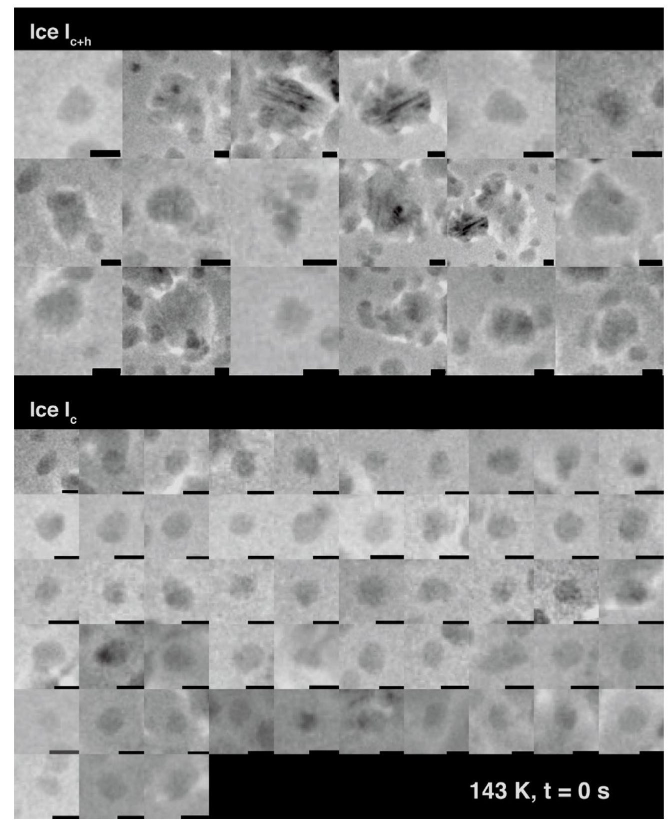

The crystalline/amorphous ice interface

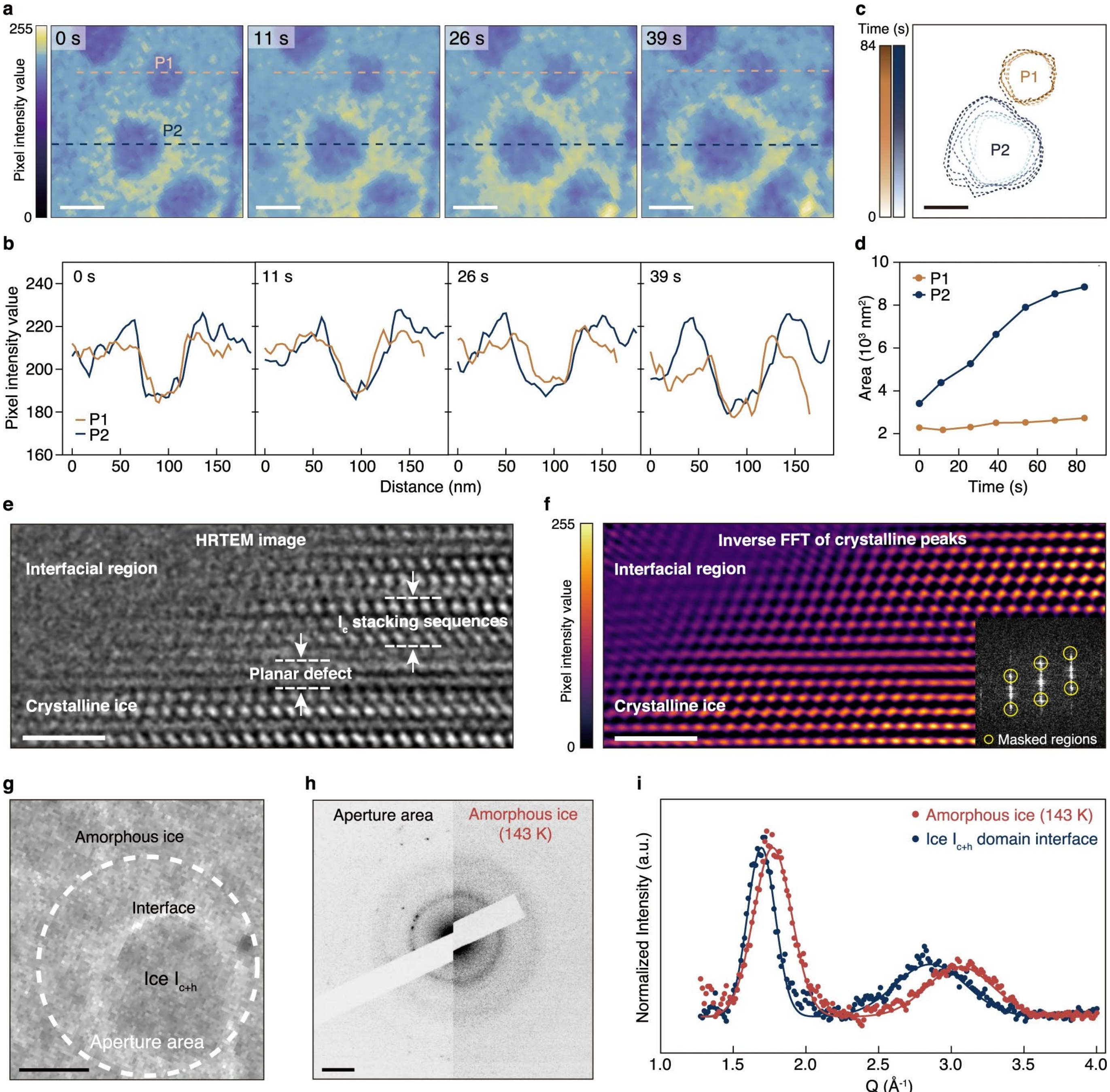

Molecular configuration properties at solid-liquid interfaces of ice polymorphs

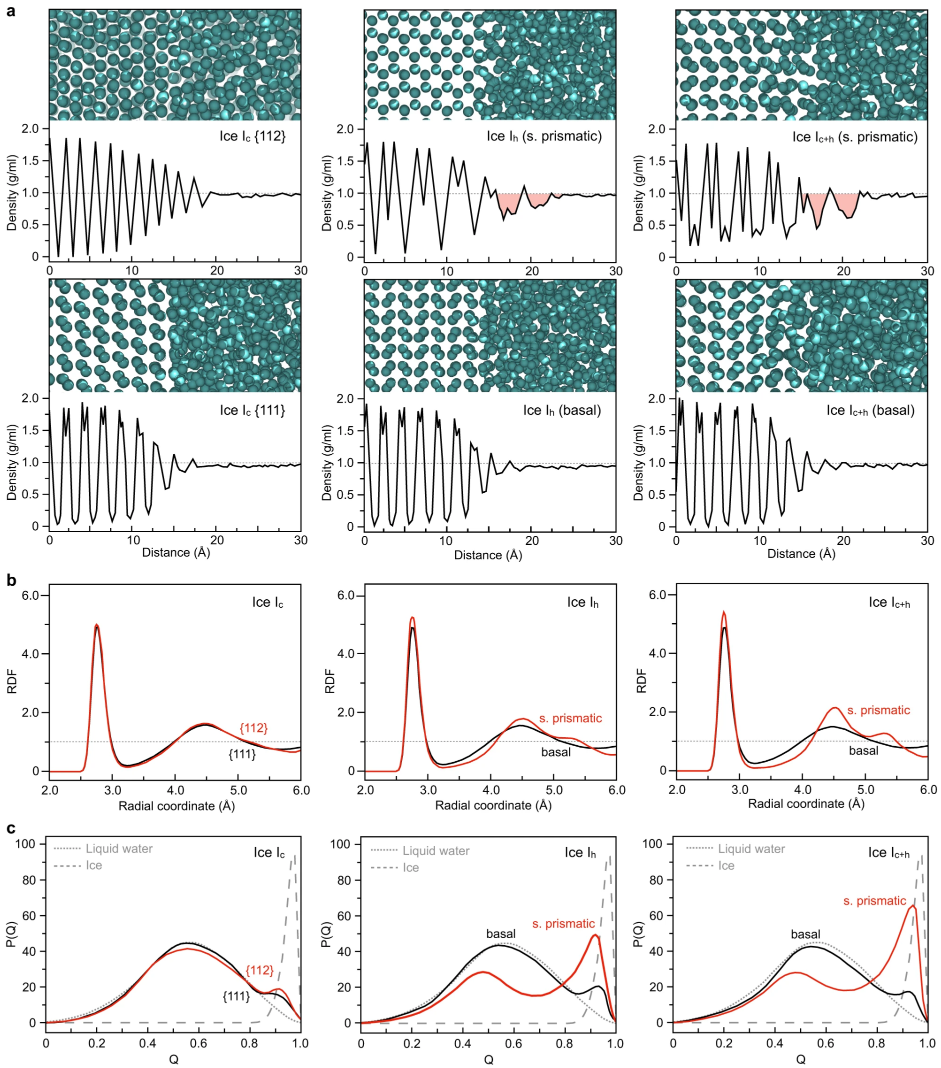

Fig. 5 | Molecular configuration properties at solid-liquid interfaces of ice polymorphs. a Molecular arrangement and density profiles of H_2O molecules at solid-liquid interfaces in proximity to ice I_c (first column), ice I_h (second column), and ice I_{c+h} (third column) in relation to the different ice planes, obtained from MD simulations. Low-density regions at the interface are emphasized with red shading. **b** Radial distribution function and **c** tetrahedral order parameter analysis of interfacial H_2O molecules adjacent to ice I_c (first column), ice I_h (second column), and ice I_{c+h} (third column) facets.

Conclusions

- Cryo-EM and MD simulations are used to track the early-stage growths of individual ice nanocrystal polymorphs in an ice film of nanoscale thickness to reveal their distinct growth dynamics and interfaces in the early stage of ice crystallization.
- I_c domains are relatively small in area and exhibit limited growth, whereas hetero-crystalline, or I_{c+h} domains undergo continual growth.
- This growth anisotropy is attributed to the distinct densities and structures of interfacial regions of growing nanocrystals.
- While water molecules near growing ice I_c crystals do not exhibit significant differences in the density or structure compared to bulk water, the fast-growing prismatic planes of ice I_{c+h} reveal the presence of a quasi-ice interface, a region that may correspond to LDL, with higher tetrahedral order and lower density than liquid water.